



Gabal El Faliq Granitoid rocks of the Southeastern Desert, Egypt: Geochemical constraints, mineralization and Spectrometric Prospecting

Gehad M. Saleh^{1*}, Doaa A. Mostafa¹, Mostafa E. Darwish¹ and Ibrahim A. Salem²

¹Nuclear Materials Authority, P. O. Box: 530 El Maadi, Cairo, Egypt

²Tanta University, Faculty of Science, Geology Department, Tanta, Egypt

*Corresponding Author E- mail: drgehad_m@ yahoo.com

Accepted 10 January, 2014

Abstract

The granitoid rocks in G. El Faliq area, southeastern Desert of Egypt, consist of granodiorites, tonalities, monzogranites and alkali feldspar granites. The G. El-Faliq area is composed of ophiolitic mélangé, gneisses, older granitoids, younger granitoids and post granitic dykes and veins. Altered granites are encountered at shears and fault zones at G. El Faliq, they rich by uranium and base metals mineralization. Geochemically, the older granitoids are peraluminous to metaluminous granites and fall in volcanic arc granites, while the younger granitoids are calc-alkaline and metaluminous to peralkaline granites and display most of the chemical characteristics of within plat granites setting. The altered granites show argillic facies with a relative depletion in K_2O and $Na_2O + CaO$ oxides. The comparison between the average of the major oxides of the fresh samples of younger granitoids related to altered ones in the studied area shows that, the younger granitoids rich in SiO_2 , Na_2O and K_2O but depleted in TiO_2 , Al_2O_3 , Fe_2O_3 , FeO , MnO , CaO , MgO and P_2O_5 related to altered ones. Also, regard to trace elements they are rich in Sr and depleted in Ni, Zn, Zr, Y, Ba, Nb, U and Th. The mineralization of G. El Faliq can be classified on the basis of mode of occurrence and lithological associations into: a) secondary uranium minerals (uranophane), b) niobium-tantalum minerals, c) sulphide minerals and d) accessory minerals. The spectrometric survey revealed the presence of enriched zones with a maximum eU content of 650 ppm and the maximum eTh is 350 ppm. The evidence of hydrothermal mineralization in the alteration of rock-forming minerals such as feldspars and the formation of secondary minerals such as uranophane and pyrite. The pre-existing primary uranium minerals are the source of the present secondary uranium minerals by the action of oxidizing fluids, mobilization of uranium and then redeposition in other forms. Redistribution by circulating meteoric waters might have taken place.

Keywords: G. El-Faliq, altered granites, uranium mineralization, spectrometric prospecting.

INTRODUCTION

The Precambrian rocks of Egypt represent the western part of the Arabian- Nubian Shield, which was formed during the Pan-African orogenic cycle (950-450 Ma, Kröner 1984) by the accretion of juvenile arc terranes, followed by crustal

thickening accompanied by intrusion of batholiths of predominantly granitic composition. Different classifications of the Egyptian granitoids were based on field relations, tectonic and geochronological determinations (El Ramly and Akaad, 1960; El Sokkary *et al.*, 1976; Akaad and Noweir, 1980; El Gaby and Habib 1982; Hussein *et al.*, 1982; El Gaby, 1975; Ragab *et al.*, 1989; Hassan and Hashad, 1990; Noweir *et al.*, 1990). Most of the younger granites are (large ionic lithosphere elements) LILE-enriched calc-alkaline to mildly alkaline rocks with I-type affinity, but some of them have been recently classified as A-type (Abdel Rahman and Martin, 1990 and Saleh, 2001). However, both I-and A-type Egyptian younger granitoids are epizonal plutons emplaced at shallow crustal levels along an active continental margin (Abdel Rahman and Martin, 1987). Several models are proposed for the origin of the Egyptian younger granites such as: 1) Partial melting of lower crust (Noweir *et al.*, 1990; Furnes *et al.*, 1996; Ibrahim *et al.*, 2001; Abd El Naby and Saleh, 2003); 2) Assimilation of pre- Pan-African old continental crust by mantle-derived mafic melts (El Gaby *et al.*, 1988 and 1990); 3) fractional crystallization of mantle-derived mafic melts (Stern and Gottfried, 1986 and Dawood *et al.*, 2005) and 4) Partial melting of an I-type granodioritic source (El-Sayed, 1998). The younger granitoids also attracted the interest of many authors because they are typically associated with anomalous concentrations of rare and some economically important elements such as Sn, W, Mo, U, Nb, Ta and Rb (Noweir *et al.*, 1990). Uranium with an average concentration of 1.0 ppm in crust needs certain geologic environments to accumulate, however, its ore deposits occur in nearly every major rock type in the crust, and nearly all igneous, metamorphic and sedimentary processes are capable of its concentration or dispersion. As the solubility of monazite and xenotime remains very low regardless of aluminosity (Pagel, 1981), phosphorus-rich peraluminous melts become saturated in monazite and xenotime at low REE concentrations. The nature abundance and distribution of accessory minerals crystallizing from melt depend on four groups of parameters (Pagel, 1981): the trace element contents (a) chemical features (b) of the magma, (c) the degree of magma evolution, (d) and the physical chemical conditions of magma crystallization. This paper presents the results of detailed investigations involving geochemistry, mineralogy and spectrometric prospecting of granitoid rocks of the G. El Faliq area to identify the mode of occurrence of mineralization.

Geological Setting and Petrography

Field Observation

Gabal (G.) El-Faliq area is located between lat. 24° 35' and 24° 42' N and long. 34° 28' and 34° 35'E. The detailed field of the basement rocks (250 Km²) is composed of ophiolitic mélangé, gneisses, older and younger granitoids and post granitic dykes and veins (Figure1).

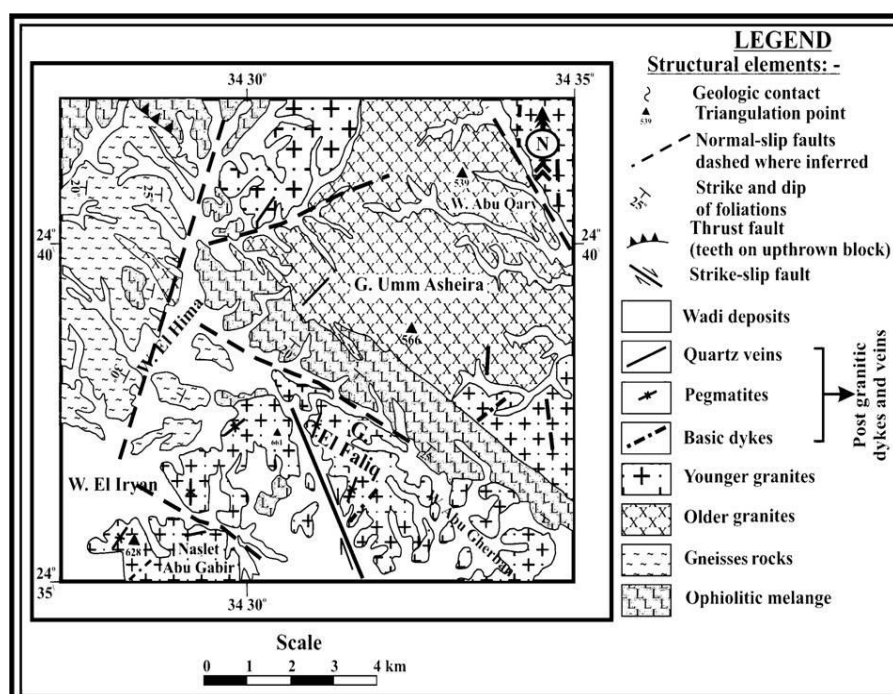


Figure 1. Geologic map of G. El Faliq area, South Eastern Desert, Egypt (Mapped by G. M. Saleh)

The older granitoids occur intruding along the contact between the ophiolitic mélangé and the younger granitoids. They are characterized by relatively low to-medium topography (Figure 2a). They are cut and crossed by number of pegmatite and quartz veins as well as basic dykes, strike 125° with dip $N 40^{\circ} E/55^{\circ}$.

The younger granitoids in G. El Faliq area exposed in the east side of the G. El Faliq, Naslet Abu Gabir as well as northeast W. Abu Gherban (about 95 km^2). They are characterized by low to moderate topography and form elongated mass in NW-SE direction. There are two varieties of younger granitoids in the study area. The first type is represented by monzogranites and alkali feldspar granites characterized by highly sheared and dissected by numerous faults (Figure 2b). The second type is represented at the eastern and northeastern sides of the regional mapped area and emplaced along NW-SE trend, reached about 1.0-2.5 Km in length and 100- 350 m in width. Some basic dikes (NE-SW) are cutting through the alkali feldspar granites (Figure 2c). Some outer contacts of younger granitoids are highly reddish colour due to the hematization (Figure 2d) or whitish due to kaolinization.



Figure 2. Photographs showing: (a) older granitoids characterized by relatively low to-medium topography, looking NE, (b) highly sheared granites and dissected by numerous faults, looking NE, (c) parallel basic dykes cut the younger granitoids, Looking NE and (d) hematitization along fractures in younger granitoids (trench No.1), looking NE, G. El Faliq area

Modal Analyses and Nomenclature

The QAP modal analysis (Streckeisen, 1976) shown in (Figure 3) indicates that the studied older granitoids are fall in the tonalite (4 samples) and granodiorite (2 samples) fields, whereas, the younger granitoids are plotted in the monzogranite (3 samples) and alkali feldspar granite (9 samples) fields. All (18) samples contain two feldspars indicating crystallization under subsolvus condition (Tuttle and Bowen, 1958).

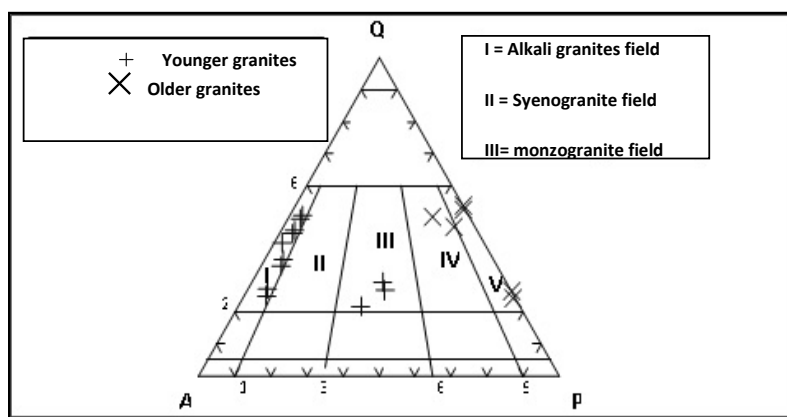


Figure 3. Modal quartz (Q) - alkali feldspar (A) - plagioclase (P) ternary diagram of the studied granitoid rocks of G. El Faliq area Streckeisen (1976)

Older Granitoids

Tonalite is medium- to coarse-grained, light gray in colour, hard and massive. They are mainly composed of plagioclase (An_{33-36}), quartz, hornblende and biotite. Apatite, zircon, titanite and opaques in order of decreasing abundance as

accessories. Plagioclase occurs as euhedral to subhedral crystals of platy and blade-like forms. It exhibits albitic twinning and zoning of normal type (Figure 4a). **Granodiorite** is medium- to coarse-grained, gray to pinkish gray colour, and exhibit hypidomorphic texture. They are mainly composed of plagioclase, quartz, orthoclase, microcline, biotite, hornblende and opaques. The accessory minerals are zircon and titanite. Plagioclase is the most dominant mineral and occurs as anhedral to subhedral prismatic crystals ranging in size from 5 x 2.6 mm to 1 x 0.2 mm. They are slightly altered, but the fresh crystals are oligoclase in composition (An_{20-26}) (Figure 4b). Accessory minerals are mainly zircon that occurs as well-euhedral crystals associating or included in the main constituents (Figure 4c).

Younger Granitoids

Monzogranite is massive, medium- to coarse-grained size, and buff to grayish buff in colour. They are mainly composed of potash feldspar, quartz, plagioclase (An_{13-20}) and biotite with subordinate amount of hornblende and muscovite. Zircon, garnet and opaques are accessory minerals. Microcline occurs as subhedral crystals showing its characteristic cross-hatched twinning (Figure 5a). Orthoclase perthite is the dominant k-feldspar, occur as anhedral to subhedral crystals (6 X 3.5 to 3 X 1.5 mm size) exhibiting patchy perthite type. Biotite occurs as pleochroic flaky crystals, with X = yellowish brown and Y = Z = dark brown (Figure 5b).

Alkali feldspar granites are medium- to coarse-grained and ranging in colour from pinkish gray to dark pink. They are mainly composed of alkali feldspars, quartz, plagioclase, alkali amphiboles. Zircon, monazite and opaques are the accessory minerals. Potash feldspars are represented by string (Figure 4d) and patchy type microcline perthite, as well as antiperthite of frequent K-feldspar exsolution in albite crystals. Potash feldspars represent by microcline and predominantly orthoclase perthite (Figure 4e). Alkali amphiboles of riebeckite-arfvedsonite represent the main mafic minerals (Figure 4f) in the alkali feldspar granites.

Altered granites are massive and moderately to strongly altered exhibiting pinkish brown to brownish red colour. They are mainly composed of alkali feldspars and quartz with subordinate plagioclases, biotite and muscovite. Zircon, monazite and opaques occur as accessories. Secondary muscovite and kaolinite as well as secondary uranium minerals generally portray irregular shapes, and coated by iron opaques (Figure 4g). The altered granites of G. El Faliq area can be categorized according to its intense hematitization (Figure 4h) and/or kaolinitization processes into hematitized and/or kaolinitized granites.

Mineralogy

The heavy minerals have been investigated by using X-ray diffraction (XRD) techniques at the Nuclear Materials Authority of Egypt. The samples were crushed and the size fraction of 0.063-0.5 mm was used. This size fraction was subjected to systematic mineral separation techniques using heavy liquids (Bromofom, 2.8 sp. gr.), magnetic fractionation using (Frantz Isodynamic Magnetic Separator) and microscopically handpicking mineral grains. The studied mineralization of G. El Faliq area can be classified into the following groups: 1) secondary uranium minerals, 2) niobium-tantalum minerals, 3) sulphide minerals and 4) accessory minerals.

Secondary Uranium Minerals

Uranophane [$Ca(UO_3)_2(SiO_2)_2(OH)_2, 5H_2O$] is one of the secondary uranium minerals which are associated with hematite, zircon and columbite-tantalite minerals. Investigating the uranophane grains under the binocular microscope showed that they are present as massive radiated and tufted aggregates as well as dense microcrystalline masses with different grades of canary to lemon- yellow colour, while it turns to the brownish yellow colour due to staining with hematite. It is identified by X-ray diffraction analyses (Figure 5a).

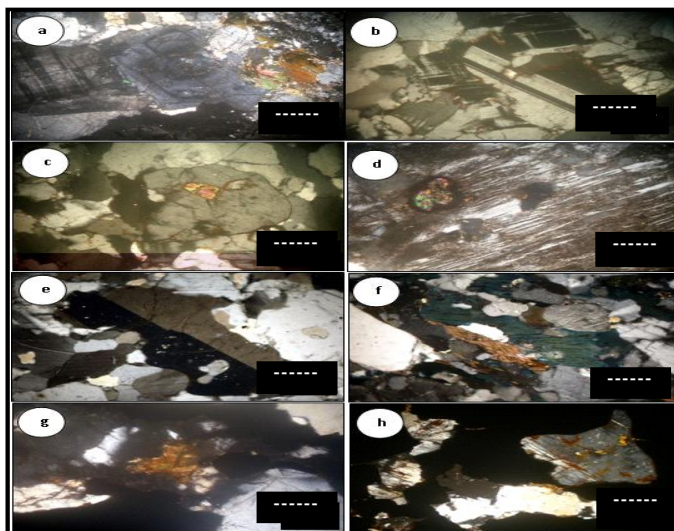


Figure 4. Thin section views in crossed nicols showing mineral assemblages and textures in the G. El-Faliq granitoid rocks: (a) euhedral plagioclase crystals showing albitic twinning and zonation in tonalite, (b) subhedral oligoclase crystals with broad lamellar twinning associating microcline in granodiorite, (c) euhedral zircon crystal included in plagioclase in granodiorite, (d) anhedral crystal of string perthite stained by iron oxides and encloses zircon in alkali feldspar granite, (e) subhedral orthoclase crystal with carlsbad twinning associating quartz in alkali feldspar granite, (f) elongated crystals of riebeckite and arfvedsonite associating quartz and perthite in alkali-feldspar granite, (g) uranophane crystal associating quartz in altered granites and (h) plagioclase corroded by iron oxides due to hematitization in altered granites

Niobium - Tantalum Minerals

Columbite [(Fe, Mn) (Nb, Ta) $2O_6$] has been recorded in altered granitic rocks of G. El Faliq area. It occurs as black colored anhedral crystals with sub-metallic to resinous luster and dark red to black streak and identified by using X-ray diffraction analysis detected the presence of columbite mineral (Figure 5b).

Euxenite [(Y, Ce, Ca, U, Th) (Nb, Ta, Ti) $2O_4$] is a brownish black mineral with a metallic luster and reddish brown streak, its fracture is concoidal to sub-concoidal. X-ray diffraction pattern of euxenite mineral is shown in (Figure 5c).

Fergusonite [(Y, Er) (Nb, Ta, Ti) O_4] is recorded in the altered granite as anhedral form with brown colour, its luster range from translucent in brown shades to glassy and the streak is grey to brown. The X-ray diffraction recorded fergusonite mineral associated with zircon (Figure 5d).

Sulphide Minerals

Pyrite (FeS_2) occurs as isometric crystals that usually appear as cubes. Pyrite has pale-brassy to golden-yellow colour with metallic luster and black streak. X-ray diffraction analysis are recorded the presence of pyrite of G. El-Faliq (Figure 6a).

Barite ($BaSO_4$) is colorless or milky white as well as greenish, reddish more yellow in colour on the periphery of the particles. X-ray diffraction analysis are recorded the presence of barite in granites of G. El-Faliq (Figure 6b).

Accessory Minerals

Allanite [(Ce, Ca, Y) (Al, Fe) $_3$ (SiO_4) $_3$.OH] is only recorded in the altered granites of G. El Faliq. It occurs as tabular, long prismatic crystals and has brown to black colour and pleochroic from pale brown to dark brown. The non metamict allanite is shown by using X-ray diffraction (Figure 7a).

Zircon ($ZrSiO_4$) is characterized by prismatic and bi-pyramidal crystals and has varying shades of honey colour due to the effect of radioactivity. Metamict zircon particles are also present, highly radioactive due to the presence of uranium and thorium. The X-ray diffraction analysis detected the presence of zircon (Figure 7b).

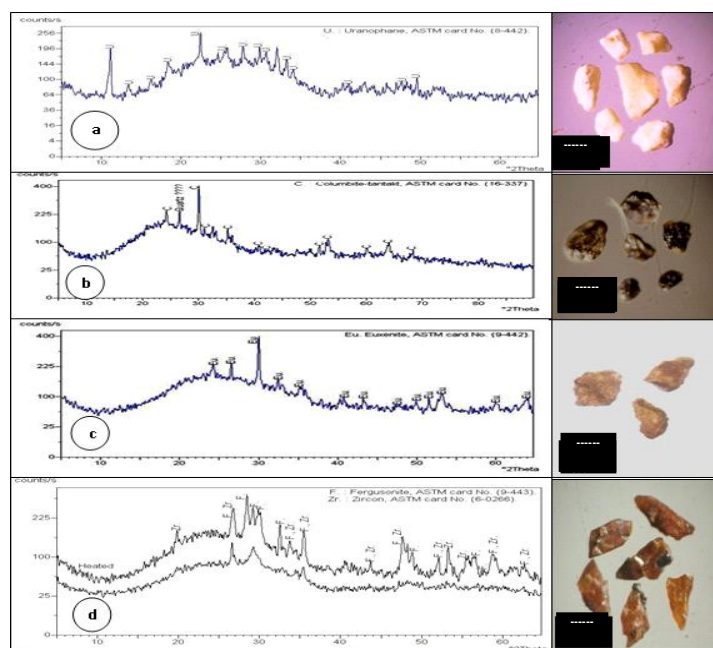


Figure 5. (a) X-ray diffractograms and photomicrographs of uranophane, (b) columbite, (c) euxenite and (d) fergusonite associated with zircon, G. El Faliq altered granites

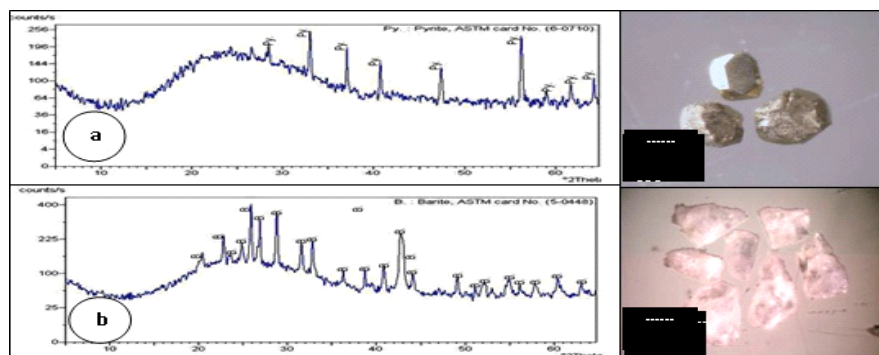


Figure 6. (a) X-ray diffractograms and photomicrographs of pyrite and (b) barite, G. El Faliq altered granites

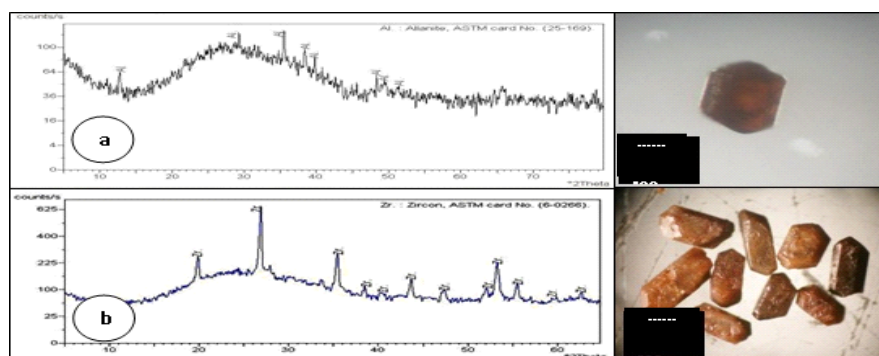


Figure 7. (a) X-ray diffractogram and photomicrograph of allanite and (b) zircon, G. El Faliq altered granites

Whole rock Geochemistry

Analytical Techniques

Twenty four (24) samples from the study area (8 alkali feldspar granites, 6 monzogranites, 5 granodiorites and 5 tonalites samples) were determined using conventional wet chemical technique (Shapiro and Brannock, 1962) for major oxides (wt%), rare earth elements ppm (REEs) and XRF technique for trace elements (ppm). The REEs were analyzed using an ICP-AES spectrometer. Absolute accuracy has been assessed by comparison with international reference materials analyzed along with the samples and is generally better than 2% for major elements and 5% for trace elements. Loss on ignition (LOI) was calculated by heating about 3g of a rock powder in a porcelain crucible at about 1000°C for 4 hours. Chemical data of the different rock types are given in Table (1).

Geochemical Classification

The studied older granitoids plot within the granodiorite and tonalite fields whereas younger granitoids samples plot in alkali feldspar granite and granite fields (Figure 8a). The normative composition Ab-Or-An ternary diagram, where the analyzed older granitoid samples fall in granodiorite and tonalite fields respectively (Figure 8b). While the younger granitoid samples located in granite field close to Ab-Or side exhibiting their low An content with slight variation of Ab-Or ratio (Barker, 1979).

Magma Type

Alumina saturation diagram (Figures 9a and b) show that the data points of the granodiorites are of metaluminous character, while tonalites fall between peraluminous and metaluminous fields. The alkali feldspar granites fall mainly in peralkaline character except one sample has peraluminous character. On the other hand, monzogranite samples fall in metaluminous field except two samples lies between peraluminous and metaluminous fields.

Table 1. Average of chemical composition of granitoid rocks of G. El-Faliq area, SED, Egypt

| Rock types | Older granitoids | | Younger granitoids | |
|---|------------------------|-------------------------|--------------------------|------------------------|
| | Granodiorites | Tonalites | Alkali feldspar granites | Monzogranites |
| No. | (N =5) | (N =5) | (N =8) | (N = 6) |
| Average and range of major oxides (wt %) | | | | |
| SiO ₂ | 65.16 (64.12-66.23) | 66.94 (65.31-69.42) | 72.01 (70.56-73.40) | 71.68 (70.70-72.70) |
| TiO ₂ | 0.93 (0.70-1.43) | 0.33 (0.002-0.50) | 0.22 (0.03-0.30) | 0.30 (0.20-0.44) |
| Al ₂ O ₃ | 14.96 14.34-15.61 | 14.776 (13.49-16.40) | 12.19 (11.83-12.60) | 12.25 (11.13-13.98) |
| Fe ₂ O ₃ | 2.094 (1.77-2.68) | 1.878 (1.54-2.68) | 1.65 (1.55-1.78) | 1.67 (0.44-2.08) |
| FeO | 2.83 (2.06-3.16) | 2.038 (1.46-2.64) | 1.59 (1.31-2.12) | 2.50 (1.80-3.32) |
| MnO | 0.07 (0.04-0.15) | 0.25 (0.07-0.90) | 0.13 (0.06-0.12) | 0.07 (0.06-0.09) |
| CaO | 3.89 (3.54-4.15) | 3.96 (3.80-4.15) | 1.25 (0.45-1.80) | 1.37 (0.80-1.90) |
| MgO | 2.76 (1.92-3.74) | 2.46 (1.90-2.83) | 0.59 (0.28-1.00) | 0.90 (0.29-180) |
| Na ₂ O | 3.45 (3.23-3.68) | 3.43 (2.88-3.86) | 4.42 (4.00-4.70) | 3.67 (3.50-3.86) |
| K ₂ O | 2.72 (2.50-3.06) | 1.25 (0.56-2.02) | 4.96 (4.33-5.23) | 4.20 (3.32-4.46) |

Table1 continuation

| | | | | |
|---|-----------------------|----------------------|---------------------|------------------------|
| P ₂ O ₅ | 0.23 (0.01-0.55) | 0.136 (0.01-0.63) | 0.07 (0.01-0.12) | 0.36667 (0.01-1.01) |
| L.O.I | 0.92 (0.70-1.45) | 0.794 (0.40-1.15) | 0.41 (0.11-0.89) | 0.67 (0.40-1.10) |
| Average and range of representative trace elements (ppm) | | | | |
| Cr | 55 (48-66) | 45 (40-53) | 56 (44-71) | 38 (31-62) |
| Ni | 6 (4-6) | 6 (5-6) | 7 (4-10) | 18 (7-31) |
| Cu | 41 (31-64) | 50.6 (46-66) | 31.25 (25-39) | 14 (10-29) |
| Zn | 168.2 (138-193) | 56 (44-63) | 52.63 (27-148) | 127 (27-205) |
| Zr | 1241.2 (1011-1663) | 82.2 (65-98) | 273 (121-831) | 1791 (1132-2792) |
| Rb | 79.8 (76-87) | 15 (14-17) | 98.38 (58-125) | 85 (42-141) |
| Y | 56.2 (44-54) | 5.6 (5-7) | 87.25 (39-254) | 164.17 (59-342) |
| Ba | 701 (670-763) | 699.6 (560-851) | 186.63 (71-550) | 374 (320-591) |
| Pb | 50.2 (44-54) | 41.4 (17-76) | 14.38 (6-31) | 13.83 (2-42) |
| Sr | 1558.4 (1164-1884) | 144 (122-174) | 361.13 (17-1437) | 667.17 (180-1956) |
| Ga | 53.8 (39-76) | 20 (6-32) | 20.75 (2-70) | 24.33 (12-28) |
| V | 9.8 (5-12) | 26 (24-30) | 4.5 (2-12) | 6.33 (6-7) |
| Nb | 57 (48-70) | 4.6 (4-6) | 35.38 (3-111) | 41 (8-151) |

AFM diagram (Figure 9c) shows that older and younger granitoid samples plot in the calc-alkaline trend. It can be noticed that the younger granitoid is closed to the alkali apex. This indicates that the studied granitoid rocks of G. El Faliq area originate from calc-alkaline magmas characteristic of orogenic belts (Irvine and Baragar, 1971).

The K₂O-Na₂O-CaO diagram (Figure 9d) to distinguish the calc-alkaline character of rocks (Condie and Hunter, 1976) and Hunter, 1979). The examined older granitoid samples plot near the CaO-Na₂O side, whereas the samples of younger granitoids plot near the K₂O-Na₂O side. Generally the all samples of the older and younger granitoids lie in calc-alkaline field of Hunter (1979).

The studied granitoid rocks fall in the I-type granite field (Figures 9e and f) except one sample of tonalite plot in S-type field according to (Chappel and White, 1974). The occurrence of magnetite and metaluminous to mildly peraluminous characters of the studied granitoids are consistent with their designation as I-type granitoids.

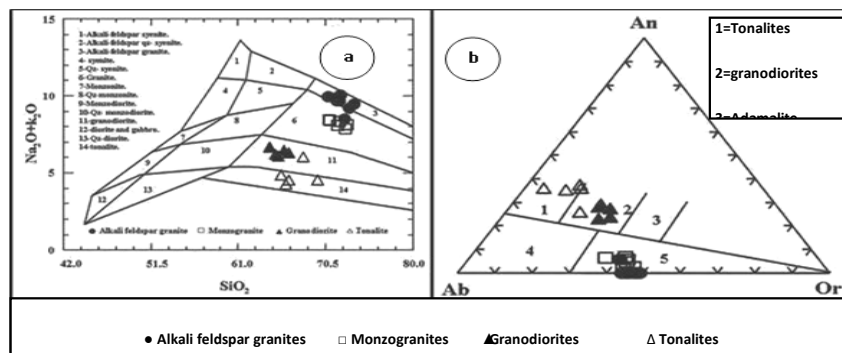


Figure 8. (a) Chemical classification of granitoid rocks using Middlemost diagram (1985) and (b) Nomenclature of granitoid rocks of Barker diagram (1979)

Potting normative Qz-Ab-Or values on the ternary diagrams (Figures 9g and h) show the water-vapor pressures up to 3K-bar after Tuttle and Bowen (1958) and 5 to 10 K-bars after Luth *et al.*(1964), whereas the diagram (Figure 9h) shows the temperature isotherms for crystallization rocks. The granitoid rocks especially the granodiorite and monzogranite fall in a relatively 2-3 K-bar and temperature ranging about 760-800°C, while tonalite fall in low water-vapor pressure ranging from 1-2 K-bar and temperature ranging about 760-840 °C indicating that, they were possibly formed at low levels in the crust. The alkali feldspar granite fall in high water-vapor pressure, varying between 3-10 K-bar and high temperature ranging about 800 °C indicating that, they were possibly formed at deep levels in the crust.

Tectonic Setting

Nb versus Y variation diagram with fields after Pearce *et al.*, (1984) is shown in (Figure 10a) the most samples of alkali feldspar granite, monzogranite and granodiorite fall within plat granites except some samples of monzogranite fall in ocean ridge granites and tonalite samples fall in volcanic arc granite. Rb versus (Nb+Y) after Pearce *et al.*(1984) variation digram. In the (Figure 10b) it can be noticed that, the most samples of alkali feldspar granite, monzogranite and granodiorite fall within plat granites and tonalite samples fall in volcanic arc granites.

Petrogenesis

The older granitoid rocks (granodiorite and tonalite) and younger granitoids (alkali feldspar granite and monzogranite) samples located between mantle line (K/Rb=1000) and core line (K/Rb=100) K/Rb diagram (Figure 10c). This indicates that the granitoid rocks of G. El Faliq area generated from source regions depleted in Rb or generated by partial melting in the lower or upper mantle, (Gast, 1965, Hart and Aldrich, 1969).

Mason (1966) reported that the average ratio K/Ba ratio for the crust is 65. The studied older granitoid rocks plot below average crustal ratio, exhibiting lower K₂O content and they have (K/Ba >65). The younger granitoid rocks located above average crustal ratio and they have (K/Ba <65), they show Ba depletion with K₂O enrichment which indicates the involvement of a second process acting with the crystal fractionation and leading to depletion of Ba with differentiation (Figure 10d).

Depletion of Sr with differentiation from the studied older granitoids toward the younger granitoid samples is shown on the Sr-Rb diagram (Figure 10e). The K/Rb ratio against Rb (Figure 10f) is useful parameters for comparing of different sources. This plot shows the same trend for all members of petrogenetic sequences of studied granitoid rocks. The curved relationships on the diagrams could suggest that crystal fractionation was the dominating process during magmatic differentiation.

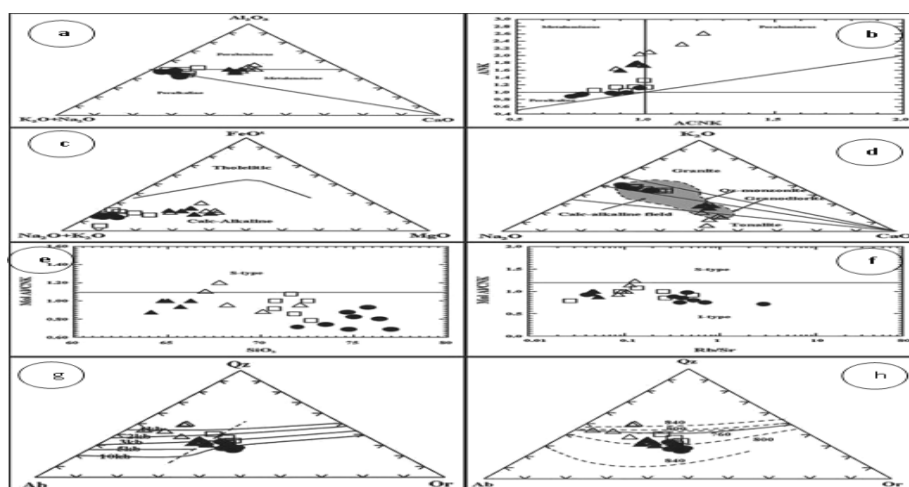


Figure 9. (a) molecular proportions of Al₂O₃-Na₂O-K₂O after Hermes *et al.*, (1978), (b) Al₂O₃/(Na₂O+K₂O) versus Al₂O₃/(CaO+ Na₂O+K₂O) diagram of Maniar and Piccoli (1989), (c) AFM diagram after (Irvine and Baragar, 1971), (f) K₂O-Na₂O-CaO diagram of Condie and Hunter (1976) and Hunter (1979), (d) Al₂O₃/(Na₂O + K₂O + CaO) ratio against SiO₂% after Chappel and White (1974), (e) Al₂O₃/(Na₂O + K₂O + CaO) ratio against Rb/Sr ratio were used by Chappel and White (1974), (f) Normative Qz-Ab-Or ternary diagram. The dashed line represents the variation in position of the minimum melting points in the granite system at different water vapor pressures and (g and h) Normative composition Qz-Ab-Or isobaric equilibrium ternary diagram after Tuttle and Bowen (1958) (Symbols as in Figure 8).

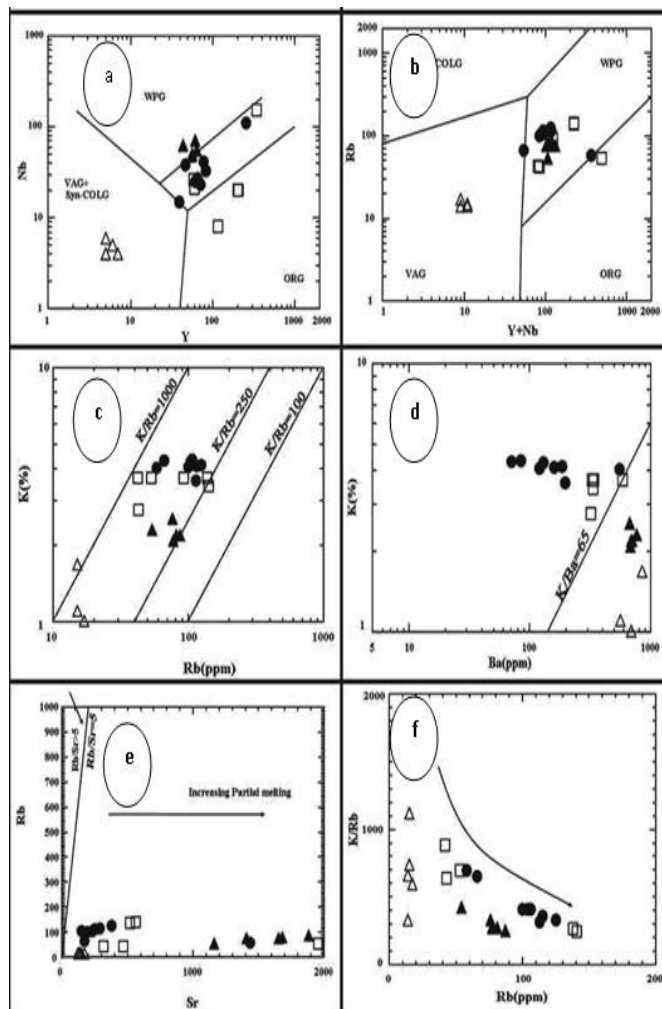


Figure 10. (a) Y versus Nb discrimination diagram (after Pearce *et al.*, 1984), (b) Rb versus (Y+Nb) discrimination diagram (Pearce *et al.*, 1984), (c) K-Rb diagram, after Shaw (1968), crustal K/Rb ratios after (Taylor, 1965), (d) Ba-K variation diagram (after Mason, 1966), (e) Sr versus Rb diagram for granitoid rocks and (f) K/Rb versus Rb diagram for granitoid rocks, (Symbols as in Figure 8).

Geochemistry of Altered Granites

The complete chemical analyses from altered granitic rocks (6 samples) are given in (Table 2). The comparison between the average of the major oxides of the fresh samples of younger granitoids related to altered ones in the studied area shows that, the younger granitoids rich in SiO_2 , Na_2O and K_2O but depleted in TiO_2 , Al_2O_3 , Fe_2O_3 , FeO , MnO , CaO , MgO and P_2O_5 related to altered ones. Also, regard to trace elements they are rich in Sr and depleted in Ni, Zn, Zr, Y, Ba, Nb, U and Th (Figures 11a and b). According to Cuney *et al.* (1989) the samples of altered granites located in argillation field (Figure 11c) toward the K-metasomatism and this consistent with formation of kaolinite minerals as product of alteration. So the argillation is represent the main alteration process affected the investigated granitic samples. Altered granite samples are plotting on AKF ternary diagram (Figure 11d) after Meyer and Hemely (1967). It shows that all samples fall in argillic field.

The weathering trends of the granitic rocks displayed on $(\text{Na}_2\text{O} + \text{CaO})\text{-Al}_2\text{O}_3\text{-K}_2\text{O}$ triangular diagram Figure (11e), Nesbitt and Young (1984 and 1989). The initial stages of weathering form a trend parallel to the $(\text{Na}_2\text{O} + \text{CaO})\text{-Al}_2\text{O}_3$ side of the diagram, whereas advance weathering shows a marked loss in K_2O compositions and more towards the Al_2O_3 apex. The Figure shows that all samples are plot toward Al_2O_3 apex and the altered granite samples are more depletion in K_2O and $\text{Na}_2\text{O} + \text{CaO}$ composition. The abundant hematite crystallization in the altered granites, which is reflected in the obvious increase of Fe_2O_3 , declares the oxidation state. The relationship of U (ppm) and the oxidation state is manifested by the ratio $\text{Fe}_2\text{O}_3 / (\text{Fe}_2\text{O}_3 + \text{FeO})$ portrayed on (Figure 11f).

Table 2. Chemical analyses of major oxides (wt. %) and trace elements (ppm) for altered granitic rocks, G. El-Faliq area, SED, Egypt

| Altered granites N = 6 | | | | | | | Average | | |
|--------------------------------|--------|--------|-------|--------|--------|--------|---------|-------|--------|
| Major Oxides | 1 | 2 | 3 | 4 | 5 | 6 | A | B | C |
| SiO ₂ | 70.84 | 69.5 | 71.5 | 68.7 | 71.02 | 69.15 | 66.05 | 71.87 | 70.12 |
| TiO ₂ | 0.34 | 0.3 | 0.4 | 0.25 | 0.31 | 0.54 | 0.63 | 0.25 | 0.36 |
| Al ₂ O ₃ | 13.23 | 12.85 | 10.3 | 12.08 | 11.12 | 13.83 | 14.87 | 12.22 | 12.24 |
| Fe ₂ O ₃ | 4.31 | 5.2 | 4.9 | 6.33 | 6.64 | 3.71 | 1.99 | 1.66 | 5.18 |
| FeO | 2.5 | 2.55 | 2.1 | 3.18 | 3.96 | 2.37 | 2.43 | 1.98 | 2.78 |
| MnO | 0.35 | 0.72 | 0.17 | 0.04 | 0.48 | 0.43 | 0.16 | 0.11 | 0.37 |
| CaO | 1.62 | 1.04 | 1.03 | 0.63 | 0.87 | 1.23 | 2.61 | 0.72 | 1.07 |
| MgO | 0.59 | 1.2 | 1 | 0.7 | 0.28 | 1.64 | 3.93 | 1.30 | 0.90 |
| Na ₂ O | 2.09 | 2.7 | 2.5 | 2.4 | 1.94 | 3.35 | 3.44 | 4.10 | 2.50 |
| K ₂ O | 4.05 | 3.5 | 3.7 | 3.1 | 3.87 | 4.33 | 1.99 | 4.63 | 3.76 |
| P ₂ O ₅ | 0.05 | 0.06 | 0.03 | 0.02 | 0.08 | 0.02 | 0.18 | 0.20 | 0.04 |
| L.O.I | 1.15 | 1.1 | 1.25 | 1.9 | 1.18 | 0.77 | 0.86 | 0.52 | 1.23 |
| Total | 101.12 | 100.72 | 98.88 | 99.33 | 101.75 | 101.37 | 99.14 | 99.56 | 100.53 |
| Trace elements (ppm) | | | | | | | | | |
| Cr | 50 | 53 | 47 | 47 | 47 | 45 | 50 | 48 | 48 |
| Ni | 223 | 228 | 140 | 518 | 588 | 549 | 6 | 11 | 374 |
| Cu | 10 | 10 | 10 | 16 | 17 | 18 | 46 | 24 | 14 |
| Zn | 157 | 156 | 121 | 361 | 367 | 368 | 112 | 85 | 255 |
| Zr | 2902 | 2782 | 1775 | >10000 | 40058 | >10000 | 662 | 923 | 21026 |
| Rb | 39 | 41 | 28 | 17 | 18 | 19 | 47 | 93 | 27 |
| Y | 1776 | 1762 | 1069 | 462 | 4744 | 4670 | 31 | 120 | 2414 |
| Ba | 685 | 699 | 646 | 1317 | 1367 | 1351 | 700 | 267 | 1011 |
| Pb | 24 | 22 | 4 | 86 | 79 | 86 | 46 | 14 | 50 |
| Sr | 57 | 55 | 34 | 23 | 22 | 23 | 851 | 492 | 36 |
| Ga | 21 | 22 | 17 | 3 | 2 | 4 | 37 | 22 | 12 |
| V | 9 | 9 | 8 | 14 | 15 | 14 | 18 | 5 | 12 |
| Nb | 3246 | 3341 | 1858 | 8611 | 8611 | 8789 | 31 | 38 | 5743 |
| U | 251 | 360 | 230 | 373 | 384 | 240 | n. d | 7 | 306 |
| Th | 252 | 548 | 414 | 571 | 439 | 432 | n. d | 8 | 443 |

A = Average of older granitoids. B = Average of younger granitoids. C = Average of altered granites. n. d. = not detected

Rare earth elements (REEs)

The average normalized REEs patterns of G. El Faliq altered granites display low to moderate fractionated REEs pattern (Figure 12) relative to chondritic values from Hasken *et al.*, (1968), where the averages $(La/Yb)_n = 2.14$ and have slight enrichment in the LREEs (1759.30), where the averages $(La/Sm)_n = 4.28$ and the average of $(Eu/Sm)_n$ is 0.38 respectively (Table 3). It is concluded that G. El Faliq altered granites have moderate negative Eu anomaly ($Eu/Eu = 0.60$), this may reflects the slight difference in their origin (Cullers and Graf, 1984). This difference can be interpreted due to the greater effect and higher oxygen activity of the melt, which is relates to volatile saturation (higher oxidation state) in case of the melt that formed the granitic melt. The oxygen activity of the melt would be sufficiently high to keep Eu at the trivalent state and thus keep its incorporation into accumulating plagioclase (Grenne and Roberts, 1998). The marked enrichment of the average of Σ HREEs (2060.91) relative to the average of Σ LREEs (1774.66) where the averages of $(Tb/Yb)_n$ recorded as 0.81 is most likely to indicate the retention of both hornblende and zircon in the source rocks relative to the melts that formed these rocks. Generally, it can be suggested that G. El Faliq altered granites are originated from different sources.

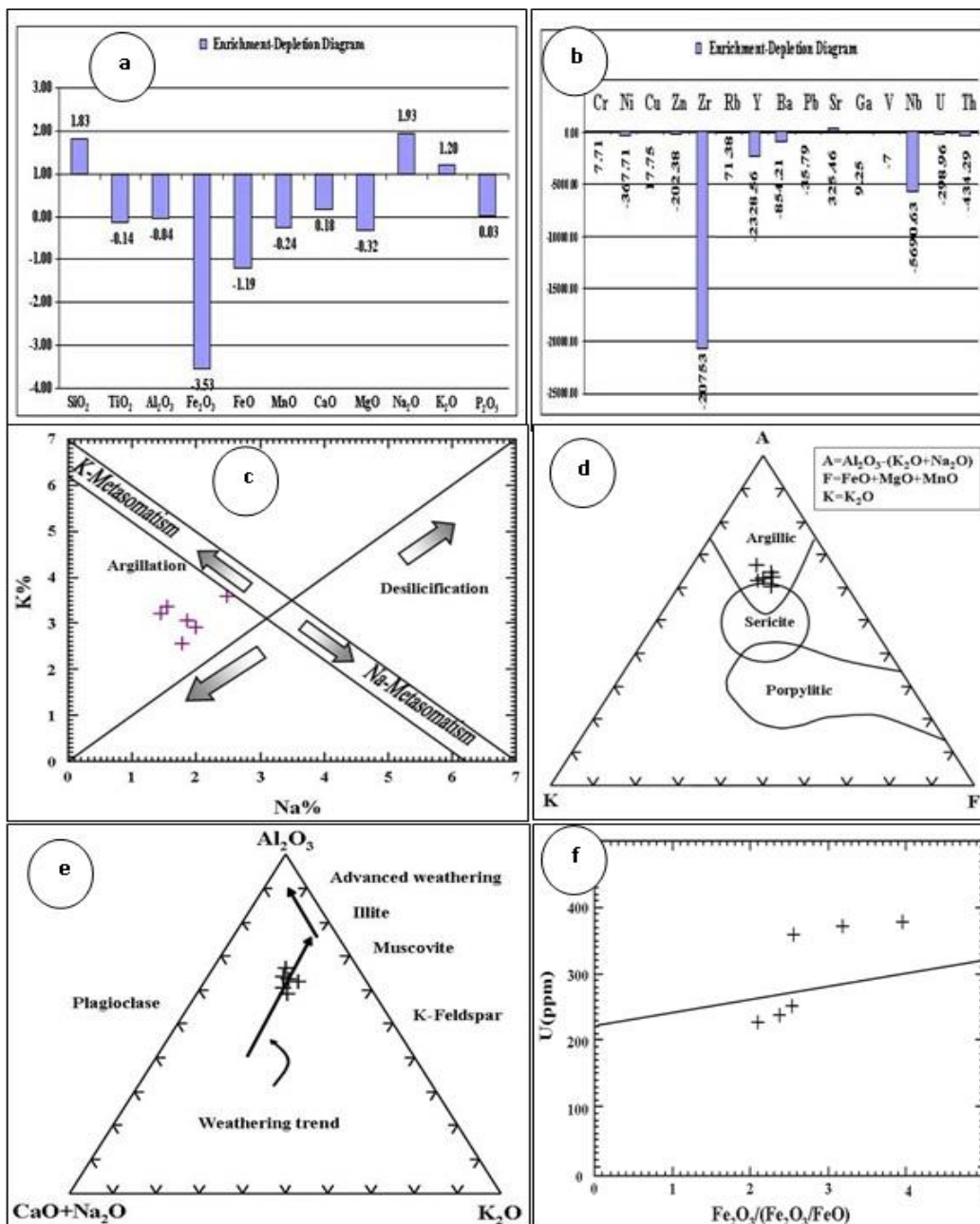


Figure 11. (a and b) The enrichment and depletion diagram in major oxides of fresh granites related to altered granites, (c) K-Na variation diagram, showing the alteration type (Cuney *et al.* 1989), (d) AKF ternary diagram (Meyer and Hemely, 1967), (e) Al₂O₃-(CaO+Na₂O)-K₂O ternary diagram, showing the weathering trend (Nesbitt and Young 1984 and 1989) and (f) U versus Fe₂O₃/(Fe₂O₃+FeO) variation diagram of the altered granites

Spectrometric Prospecting

In situ γ -ray spectrometry measurements have been carried out using a UG-512 spectrometer with a 3 x 3 sodium iodide (Thalium) [NaI(Tl)] crystal detector. Before field measurements the spectrometer is calibrated on concrete pads containing known concentrations of K, U and Th. This calibration provides for correction of the measured K, eU and eTh. The term "equivalent" or its abbreviation "e" is used to indicate that equilibrium is assumed between the radioactive daughter isotope monitored by the spectrometer, and its relevant parent isotope. γ -rays emitted by ²¹⁴Bi at 1.76 MeV were measured for ²³⁸U and gamma rays emitted by ²⁰⁸Tl at 2.41 MeV were measured for ²³²Th. Within the detector, an internal ¹³⁷Cs source allows the spectrometer to automatically maintain system stability is measured over a large body of water.

Distribution of Radio-elements in Granitoid Rocks

The total count (Tc), eU, eTh, eU/eTh, eTh/eU and K% in the younger granitoids rocks and altered granites (shear zone I and shear zone II) of G. El Faliq area respectively. The relation between the eU, eTh contents, eU/eTh and eU - (eTh/3.5) among the younger granitoids indicate slightly positive correlation while the variation between the eU/eTh ratios and eTh contents (Fig.13) shows negative linear correlation suggests enrichment of uranium relative to thorium that indicate uranium had been added to these granitoids. While, the relationship between eU with eTh, the eU with eU/eTh contents and eU - (eTh/3.5) among the altered granites reflect a direct relation (Figs.14 and 15), while the relation between eTh and eU/eTh and the eU with K% shows random and negative linear distribution, that means the eU/eTh ratio tends to increase with uranium mobilization and post magmatic redistribution in anomalies shear zones I and II of G. El Faliq, uranium had been added to these granites and this could be a favorable economic criterion into zones with the G. El Faliq area (Boyle, 1982).

Equilibrium State of Radioactive Anomalies

The D-factor (U/eU) is equal to the ratio of the chemically determined uranium/radiometrically measured uranium (Hansink, 1976). If this factor is approximately unity, it indicates addition or removal of uranium respectively (Stuckless *et al.*, 1984). From the D-factor of the G. El Faliq samples of the altered granites presented in Table (4) and (Figure 16), it is clear that chemical uranium is less than the radiometric uranium in all of the samples, which reflects disequilibrium due to the removal of uranium.

Table 3. The REEs contents of the altered granitic rocks, G. El Faliq area, SED, Egypt

| Altered granites | | | | | | | |
|----------------------|--------|---------|---------|--------|---------|---------|---------|
| Samples | 1 | 2 | 3 | 4 | 5 | 6 | Average |
| La | 32.75 | 796 | 285.15 | 15.42 | 158.95 | 405.71 | 282.33 |
| Ce | 110.3 | 1765.95 | 646.5 | 45.44 | 378.4 | 905.70 | 642.05 |
| Pr | 19.35 | 209 | 74.8 | 4.2 | 47.08 | 106.6 | 76.84 |
| Nd | 93.72 | 2029 | 510.35 | 13.5 | 302.04 | 1021.25 | 661.64 |
| Sm | 34.2 | 259.18 | 90.85 | 1.55 | 62.53 | 130.37 | 96.45 |
| Eu | 4.5 | 42.8 | 13.9 | 0.2 | 9.2 | 21.5 | 15.35 |
| Gd | 141.65 | 523.5 | 141.05 | 3.2 | 141.35 | 263.35 | 202.35 |
| Tb | 42.01 | 187.68 | 38.32 | 0.56 | 40.17 | 94.12 | 67.14 |
| Dy | 238.65 | 1571.1 | 303.65 | 4.47 | 271.15 | 787.79 | 529.47 |
| Ho | 56.3 | 446.61 | 95.95 | 1.1 | 76.13 | 223.86 | 149.99 |
| Er | 157.1 | 1219.54 | 188.88 | 3.45 | 172.99 | 611.50 | 392.24 |
| Tm | 21.95 | 141.72 | 28.4 | 0.42 | 25.18 | 71.07 | 48.12 |
| Yb | 128.6 | 1177.5 | 150.3 | 2.7 | 139.45 | 590.1 | 364.78 |
| Lu | 15.5 | 1197.7 | 13.65 | 0.41 | 14.58 | 599.06 | 306.82 |
| ∑ REEs | 1097.6 | 11569.3 | 2584.8 | 100.6 | 1841.17 | 5834.95 | 3838.06 |
| ∑ LREEs | 294.82 | 5101.93 | 1621.55 | 80.31 | 958.2 | 2591.13 | 1774.66 |
| ∑ HREEs | 801.76 | 6465.35 | 960.2 | 16.31 | 880.98 | 3240.83 | 2060.91 |
| LREEs/HREEs | 0.36 | 0.78 | 1.67 | 4.91 | 1.015 | 2.85 | 1.93 |
| (La/Yb) _n | 0.25 | 0.68 | 1.9 | 5.71 | 1.08 | 3.20 | 2.14 |
| (La/Sm) _n | 0.96 | 3.07 | 3.14 | 9.95 | 2.05 | 6.51 | 4.28 |
| (Gd/Lu) _n | 9.14 | 0.44 | 10.33 | 7.8 | 9.74 | 4.12 | 6.93 |
| (Gd/Yb) _n | 1.1 | 0.44 | 0.94 | 1.19 | 1.02 | 0.82 | 0.92 |
| (Tb/Yb) _n | 0.15 | 0.72 | 1.16 | 0.94 | 1.31 | 0.72 | 0.81 |
| (Eu/Sm) _n | 0.35 | 0.44 | 0.40 | 0.34 | 0.39 | 0.34 | 0.38 |
| (Eu) _n | 77.59 | 737.93 | 239.66 | 3.4 | 158.62 | 370.69 | 264.64 |
| Eu* | 392.52 | 317.83 | 638.4 | 157.75 | 530.2 | 1044.97 | 514.61 |
| Eu/ Eu* | 0.20 | 2.32 | 0.38 | 0.02 | 0.30 | 0.35 | 0.60 |

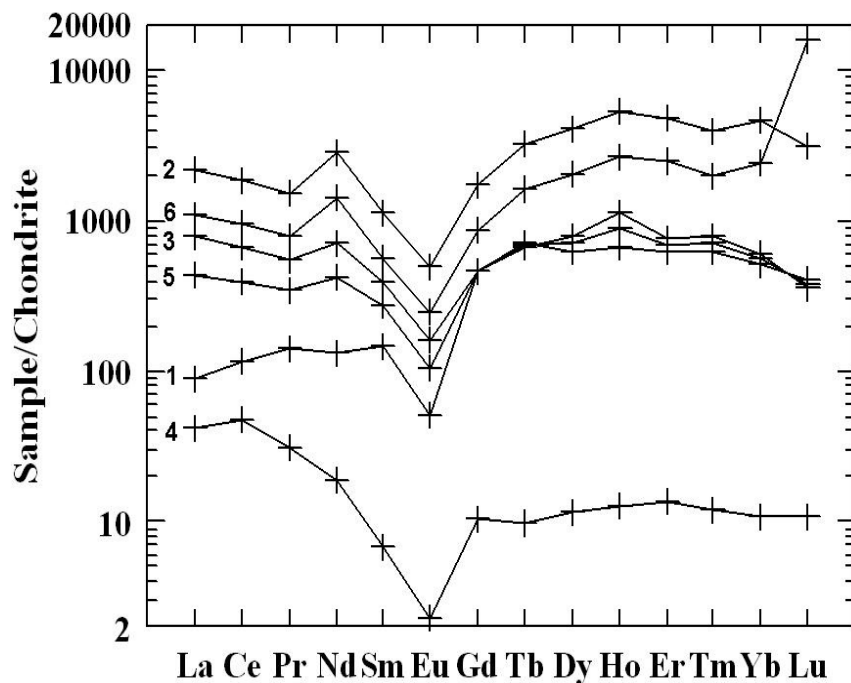


Figure 12. Chondrite normalized REEs abundances in the studied altered granitic rocks using the normalizing values of (Hasken *et al.*, 1968)

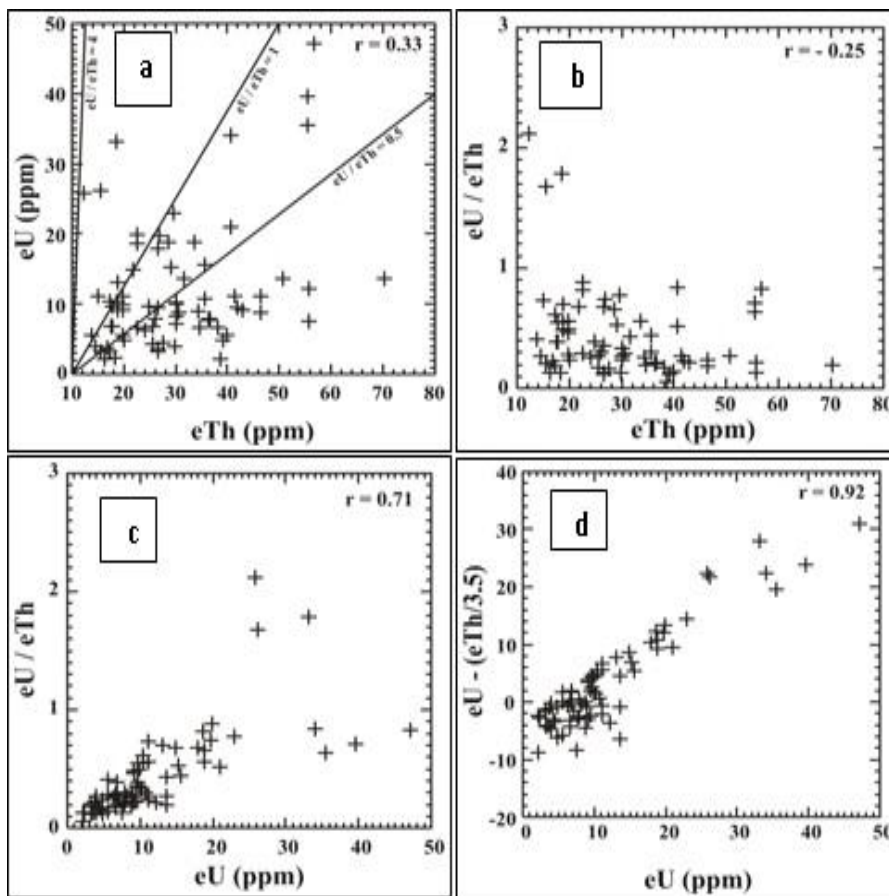


Figure 13. The relation between: (a) $eU - eTh$, (b) $eTh - eU/eTh$, (c) $eU - eU/eTh$ and (d) $eU - (eTh/3.5)$ of younger granitoids, G. El Faliq , SED, Egypt

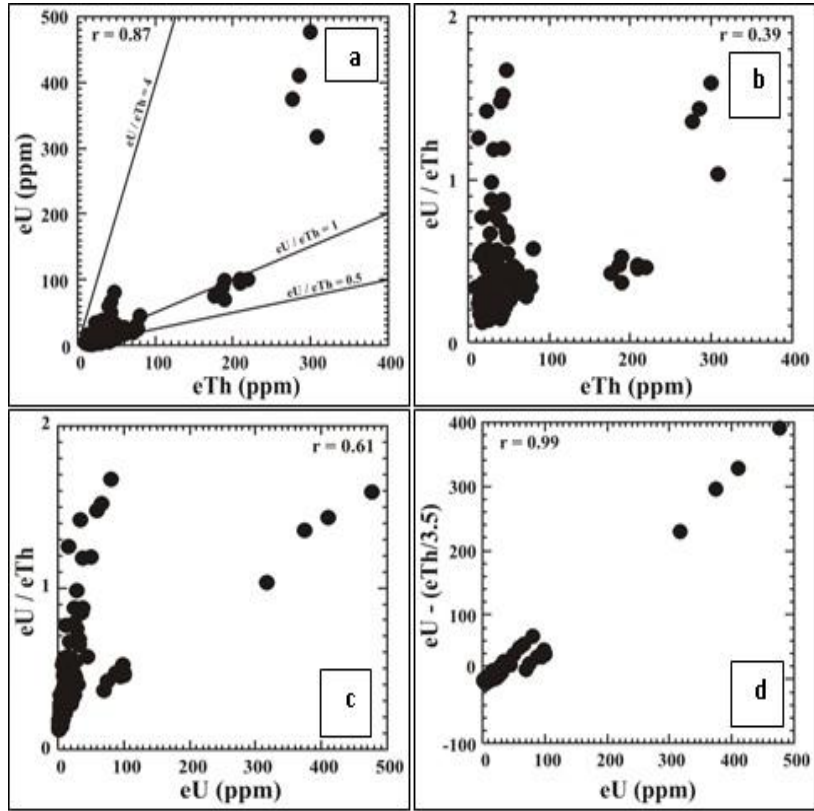


Figure 14. The relation between (a) eU - eTh, (b) eTh - eU/eTh, (c) eU - eU/eTh and (d) eU- (eTh/3.5) of altered granites (Shear zone I), G. El Faliq area, SED, Egypt

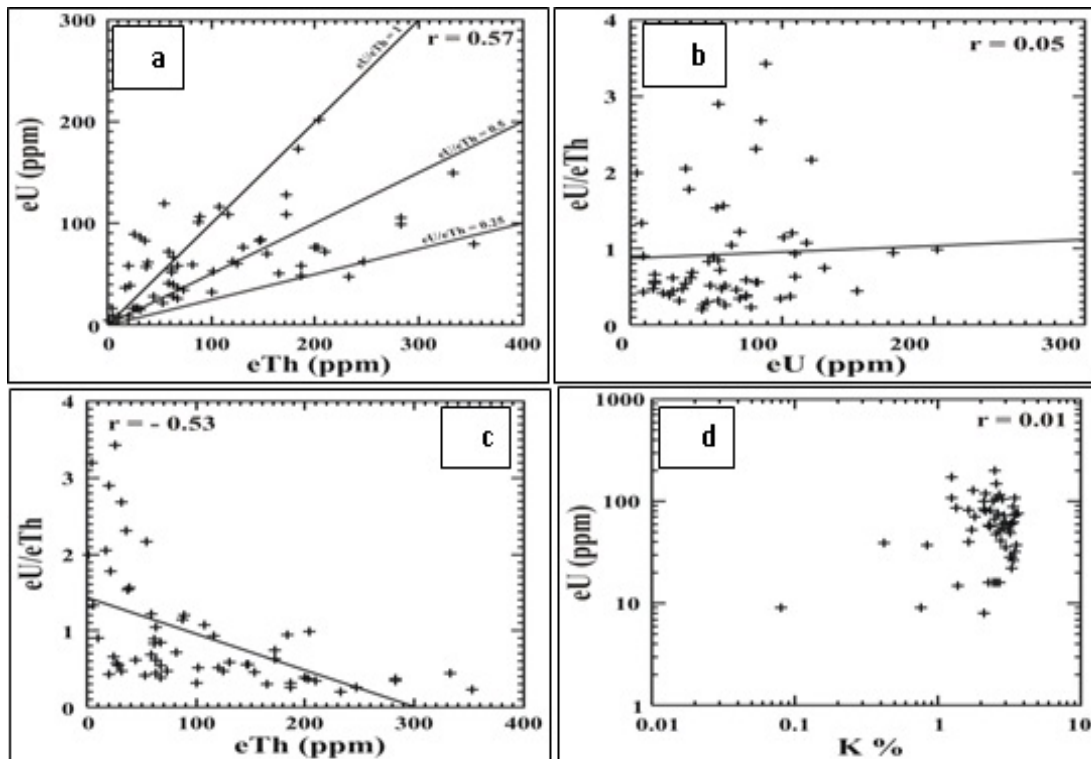
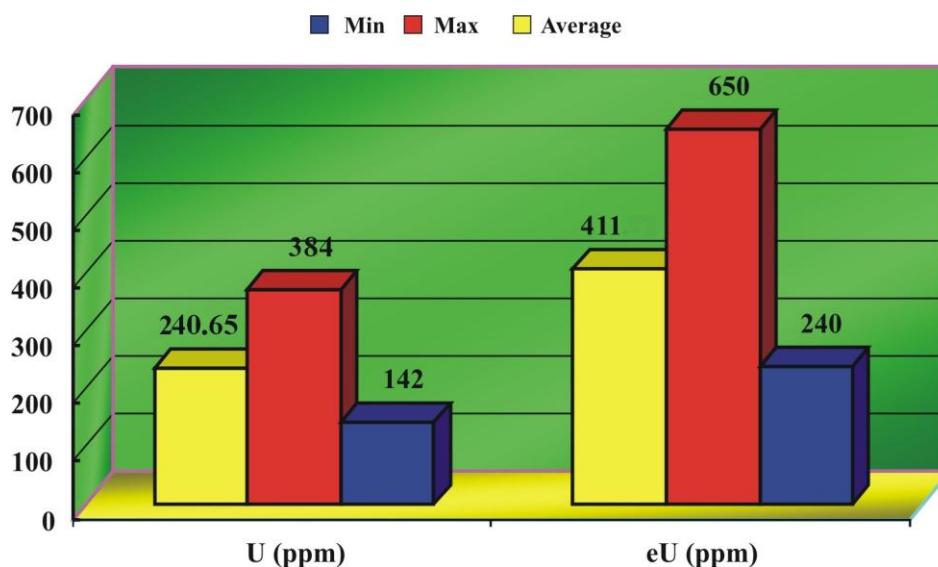


Figure 15. The relation between (a) eU - eTh, (b) eU - eU/eTh, (c) eTh - eU/eTh and (d) K-eU of altered granites (Shear zone II), G. El Faliq area

Table 4. Results of U-spectrometric (eU) and U- chemical analyses of G. El Faliq altered granites, SED, Egypt

| Sample No | eU (ppm) | U (ppm) | U/eU | Sample No | eU (ppm) | U (ppm) | U/eU |
|-----------|----------|---------|------|-----------|----------|---------|------|
| 1 | 510 | 251 | 0.49 | 11 | 345 | 225 | 0.65 |
| 2 | 590 | 360 | 0.61 | 12 | 330 | 220 | 0.67 |
| 3 | 350 | 230 | 0.66 | 13 | 240 | 147 | 0.61 |
| 4 | 650 | 373 | 0.57 | 14 | 280 | 142 | 0.51 |
| 5 | 390 | 384 | 0.98 | 15 | 390 | 235 | 0.60 |
| 6 | 380 | 240 | 0.63 | 16 | 470 | 220 | 0.47 |
| 7 | 270 | 150 | 0.56 | 17 | 485 | 233 | 0.48 |
| 8 | 295 | 210 | 0.71 | 18 | 520 | 264 | 0.51 |
| 9 | 265 | 149 | 0.56 | 19 | 610 | 311 | 0.51 |
| 10 | 300 | 227 | 0.76 | 20 | 550 | 242 | 0.44 |

**Figure 16.** Bar diagram showing the comparison between average of U-chemistry (ppm) and U-radiometry (ppm) G. El Faliq altered granites

CONCLUSIONS

1. The G. El-Faliq area is composed of ophiolitic mélangé, gneisses, older and younger granitoids and post granitic dykes and veins. The younger granitoids exposed in the east side of the G. El Faliq area especially in Naslet Abu Gabir and northeast W. Abu Gherban. Petrographically, they are mainly composed of potash feldspar, quartz, plagioclase, biotite and hornblende. Accessory minerals are represented by zircon, garnet and opaques. Altered granites are characterized by intense hematitization and kaolinization. Microscopically, they are mainly composed of alkali feldspars and quartz with subordinate plagioclases, biotite and muscovite. Zircon and opaques in addition to monazite occur as accessories.

2. Geochemically, the older granitoids are peraluminous to metaluminous granites, while the younger granitoids are calc-alkaline and metaluminous to peralkaline granites. The altered granites show argilic facies with a relative depletion in K_2O and $Na_2O + CaO$ oxides. The average normalized REEs patterns of altered granites display low to moderate fractionated REEs pattern relative to chondritic values from Hasken *et al.* (1968). Generally, it can be suggested that G. El Faliq altered granites are originated from different sources.

3. The mineralization of G. El Faliq can be classified on the basis of mode of occurrence and lithological associations into: a) secondary uranium minerals (uranophane), b) niobium-tantalum minerals (columbite, euxenite and fergusonite), c) sulphide minerals (pyrite and barite) and d) accessory minerals (allanite and zircon) as confirmed by XRD analysis.

4. The radiometric investigation suggested that the studied granitoid are uraniumiferous granites, which were considered as favorable environments for uranium deposition containing high eU and eTh. The origin of secondary uranium mineralization is mainly related to alteration of primary minerals by the action of oxidizing fluids, mobilization of uranium and then redeposition in other forms. Redistribution by circulating meteoric waters might have taken place.

ACKNOWLEDGMENTS

The authors wishes to thanks the Prof. Dr. M. E. Ibrahim, Head of the Research Sector, Nuclear Materials Authority, Egypt and Dr. Magda A. Khalaf for interest as well as for help during field work and for guidance during the progress of the manuscript.

References

- Abd El Naby HH, Saleh GM (2003). Radioelement distributions in the Proterozoic granites and associated pegmatites of Gabal El Fereyid area, Southeastern Desert, Egypt. *Applied Radiation and Isotopes*. 59: 289-299.
- Abdel RAM, Martin RF(1987). Late-Pan African magmatism and crustal development in northeastern Egypt. *Geol. J.* 22:281-301.
- Abdel RAM, Martin RF(1990). The Mount Gharib A-type granite, Nubian Shield: petrogenesis and role of metasomatism at the source. *Contrib. Miner. and Petro.* 104:173-183.
- Akaad MK, Noweir AM (1980). Geology and lithostratigraphy of the Arabian Desert orogenic belt of Egypt between lat. 25 35 and 26 30 N. *Inst. Applied Geol., King Abdul Aziz Univ., Jeddah* 3(4): 127-135.
- Barker F(1979). Trondhjemite definition, environment and hypotheses of origin. In Barker (ed.): *Trondhjemite, dacites and related rocks. Developments in Petrology*, El Sevier Publishing Co., Amsterdam. 6:1-12.
- Boyle RW(1982). Geochemical prospecting for thorium and uranium deposits. *Develop. Economic, geol.*, 16, El Sevier, Amsterdam. Pp.189.
- Chappell BW, White AJR (1974). Two contrasting granite types: *Pacific Geol.*, 8:284-293.
- Condie, K. C., and Hunter, D. R., 1976: Trace element geochemistry of Archean granitic rocks from the Barberton region, South Africa. *Earth Planet Sci.* 29: 389 – 400.
- Cullers RL, Graf L(1984). Rare earth elements in igneous rocks of the continental crust: intermediate and silicic rocks ore petrogenesis. In: Henderson, p. (ed.), *Rare earth element geochemistry*. El Sevier, Pub. Co., Amsterdam. 2:275-316.
- Cuney M, Leroy J, Volivezo A, Daziano C, Gambda B, Zarco AJ, Morello O, Ninci C, Molina P(1989). Metallogenesis of the uranium mineralized Achala granitic complex, Argentina: comparison with Hercynian peraluminous leucogranites of Western Europe. *Proc. Tech. Comm. Meetings, Vienna, TECDOC-543, I.A.E.A., Vienna*. Pp. 211 - 232.
- Dawood YH, Saleh GM, Abd El Naby HH(2005). Effects of hydrothermal alteration on Geochemical characteristics of the El Sukkari granite, central Eastern Desert, Egypt. *International Geology Review*. 47: 1316-1329.
- El Gaby S(1975). Petrochemistry and geochemistry of some granite from Egypt. *Neues Jahrbuchfur Mineral*. 124:147 – 189.
- El Gaby S, Habib MS (1982). Geology of the area SW of Port Safaga, with especial emphasis on the granitic rocks, Eastern Desert, Egypt. *Ann. Geol. Surv. Egypt*. 12: 47 – 71.
- El Gaby S, List FK, Tehrani R (1990). The basement complex of the Eastern Desert and Sinai". In (Said, R. ed.) *The Geology of Egypt*. Balkama-Rotterdam Brookfield. Pp.175-184.
- El Gaby S, List FK, Tehrani R(1988). Geology, evolution and metallogenesis of the Pan-African Belt in Egypt. In (S.El Gaby, S and R.D.Greiling, R.D., eds). *The Pan-African Belt of the North East Africa and Adjacent Areas*. Vieweg Verlag, Wiesbaden. Pp. 17-68.
- El Ramly MF, Akaad MK(1960) The basement complex in the Central Eastern Desert of Egypt between latitudes 24° 30 and 25° 4^N *Geol. Surv. Egypt*. 8:35.
- El Sayed MM (1998). Tectonic setting and petrogenesis of the Kadabora pluton: A late Proterozoic anorogenic A-type Younger Granitoids; *Chem. Erde*. 58: 38-63.
- El Sokkary AA, El Shatoury HM, Sayyah TA, Attawiya MY, Assaf HS(1976). Contribution to the geochemistry of some granitic rocks from Egypt. *Erde*. 35:335-343.
- Furnes H, El Sayed MM, Khalil SO, Hassanen MA(1996). Pan-African magmatism in the Wadi El Imra district, Central Eastern Desert, Egypt: geochemistry and tectonic environment; *Jour. Gol. Soc. Lond*. 153: 605-818.
- Gast PW (1965). Terrestrial ratio of potassium to rubidium and composition of the earth's mantle. *Science*. 147:858-860.
- Grenne T, Roberts D(1998). The Holonda porphyrite, Norwegian Caledonides: geochemistry and tectonic setting of Early-Mid. Ordovician shoshonite volcanism. *J. Geol. Soc., London*. 155:131-142.
- Hansink JP(1976). Equilibrium analysis of sandstone rollfront uranium deposits. *Proceedings Inter. Symposium on exploration of uranium deposits*. Int. Atomic Energy Agency, Vienna. Pp. 683 - 693.
- Hart SR, Aldrich LT(1969) Fractionation of potassium/rubidium by amphiboles: Implications regarding mantle composition. *Science*. 155:325-327.
- Hasken LA, Haskin MA, Frey FA, Wildman TR (1968). Relative and absolute terrestrial abundance of the rare earths. In: Ahrens L. H. (ed.), *Origin and distribution of the elements*, vol. 1. Pergamon, Oxford. Pp. 889 - 911.
- Hassan MA, Hashad AH(1990) Precambrian of Egypt. In: Said R. (ed): *The Geology of Egypt*. Balkema, Rotterdam. Pp. 201-245.
- Hermes OD, Ballard RD, Banks PO (1978). Upper Ordovician peralkalic granites from the Gulf of Maine., *Geol. Soc. Am. Bull.* 89:1761-1774.
- Hunter DR (1979). The role of tonalitic and trondhjemitic rocks in the crustal development of Swaziland and the Eastern Transvaal, South Africa. In: Barker, F. (ed.): *Trondhjemites, dacites and related rocks*. Elsevier, Amsterdam. Pp. 303 - 322.
- Hussein AA, Ali MM, El Ramly MF(1982). A proposed new classification of the granites of Egypt; *Jour. Volcan. Geoth. Res*. 14: 187-198.
- Ibrahim ME, Saleh GM, Abd El Naby HH (2001) Uranium mineralization in the two mica granite of Gabal Ribdab area, South Eastern Desert, Egypt. *Applied Radiation and Isotopes*. 55: 861-872.
- Irvine TN, Baragar WRA (1971). A guide to the chemical classification of the common volcanic rocks. *Can. J. Earth Sci.* 8:523-548.
- Kröner A(1984). Late Precambrian plate tectonics and orogeny: a need to redefine the term Pan-African. In (Klerkx, J. and Michot, J. eds.) *Geologie Africane. African Geology*. Pp. 23-28.
- Luth WC, Jams RH, Tuttle OF (1964). The granite system at pressure of 4 to 10 kilobars. *J. Geophys. Res.* 69: 759-773.
- Maniar PD, Piccoli PM(1989) Tectonic discriminations of granitoids. *Geol. Soc. Amer. Bull.* 6: 129 -198.
- Mason D (1966). *Principals of geochemistry*. 3rd (ed.), Wiley and Sons, New York. Pp. 310.
- Meyer C, Hemley JJ (1967). Wall rock alterations, 166 – 235. *Geochemistry of hydrothermal ore deposits* (H. G. Barnes, ed.), Winston Inc. New York. Pp. 670.
- Middlemost EAK (1985). *Magma and magmatic rocks.*, Longman, London.
- Nesbitt HW, Young GM (1989). Formation and diagenesis of weathering profiles. *J. Geol.* 97:129 – 147.
- Nesbitt HW, Young GM(1984). Prediction of some weathering trends of plutonic and volcanic rocks based up on thermodynamic and kinetic consideration. *Geochim. Cosmochim. Acta.*, 48: 1523 – 1534.

- Noweir AM, Sewifi BM, Abu El Ela AM (1990). Geology, petrography, geochemistry and petrogenesis of the Egyptian younger granites. *Qatar Univ. Sci. Bull.*, 10:363-393.
- Pagel M (1981). The mineralogy and geochemistry of uranium, thorium, and rare-earth elements in two radioactive granites of the Vosges, France. *Mineral. Mag.*, 46:149-161.
- Pearce JA, Harris NBW, Tindle AG (1984). Trace element discrimination diagrams for the tectonic interpretation of granitic rocks. *J. Petrol.* 25: 956 – 983.
- Ragab AI, Meneisy MY, Diab MM (1989). Petrology and petrogenesis of the older and younger granitoids of Wadi Bezah area, Central Eastern Desert, Egypt. *Jour. Afr. Earth. Sci.* 9(2): 303-315.
- Saleh GM (2001). Evolution of Pan-African A- and I-type granites from south eastern Desert, Egypt: Inferences from geology, geochemistry and mineralization; *International Geology Review.* 43: 548-564.
- Shapiro L, Brannock WW (1962). Rapid analysis of silicate, carbonate and phosphate rocks, U. S. Geol. Surv. Bull, 114 A, Pp.56.
- Shaw DM (1968). A review of K/Rb fractionation trends by covariance analysis. *Geochim. Cosmochim., Acta.* 32, :573-601.
- Stern RJ, Gottfried DY (1986). Petrogenesis of late Precambrian (575-600 Ma) bimodal suite in north-east Africa; *Contrib. Miner. and Petr.* 92: 492-501.
- Streckeisen A (1976). "To each plutonic rock its proper name". *Earth Science Reviews.* 12: 1-33.
- Stuckless JS, Nkomo IT, Winner DB, Van Trump G (1984). Geochemistry and uranium favourability of the postorogenic granites of the north-eastern Arabian Shield, Kingdom of Saudi Arabia, and *Bull. Fac. Earth Sci., King Abdel Aziz Univ.* 6:195 – 209.
- Taylor SR (1965). The application of trace element data to problems in petrology, in *physical and chemistry of the Earth.* Editors, Ahrens, L.H., Press, F, Runcor, S. K., and Urey, H. C., Pp. 133 – 213.
- Tuttle OF, Bowen NL (1958). Origin of granite in the light of experimental studies in the system $\text{NaAlSi}_3\text{O}_8\text{-KAlSi}_3\text{O}_8\text{-SiO}_2\text{-H}_2\text{O}$. *Geol. Soc. Am. Em.* 74:153.